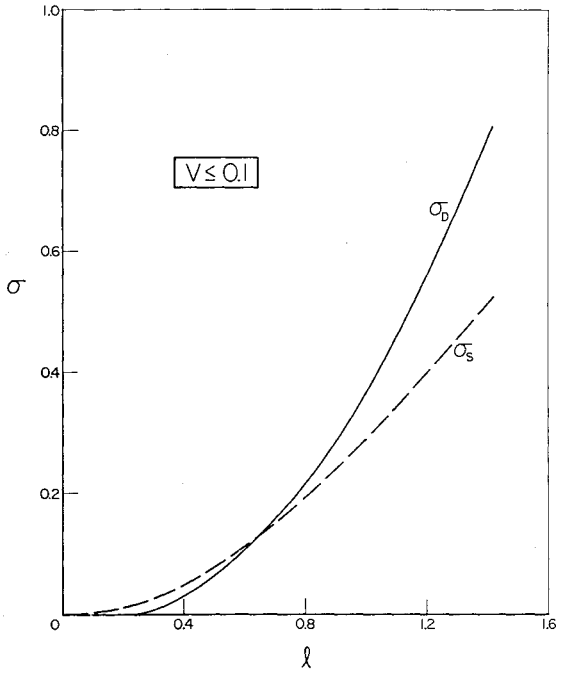

Fig. 2 Dependence of tangential momentum accommodation coefficient on l for $V \leq 0.1$.

$\theta'(x,\theta)$ can be determined analytically from the trajectory geometry for given values of the size ratio $l \equiv L/d$.

The evaluation of the slip velocity and surface shear stress was done numerically using an IBM 7040/7094 computer, and the results are given in Table 1 and Fig. 2 for thirty $l - V$ pairs. The slip velocity and shear stress are presented in terms of the slip coefficient $C_s = u_s/U$ and the drag coefficient $C_D = \tau_s/\frac{1}{2}\rho_0 U^2$. The tangential momentum accommodation coefficient σ is related to C_s and C_D by[7] $\sigma \equiv \sigma_s = 2(1 - C_s)$ and $\sigma \equiv \sigma_D = \pi^{1/2} V C_D$. Finally, as shown in Fig. 1, a given collisional trajectory can involve either one or two impact points, depending on the values of x, θ and l [for $l \leq (2)^{1/2}$]. The integrals in Eqs. (3) were separated into contributions from the two cases, and f_1, the fraction of *molecules* which undergo only one impact, and F_1, the fraction of the *collision rate* involving one impact, were computed.

The significance of the trends in the results is generally evident from Table 1, but a few observations seem worthy of emphasis. For low plate velocities, i.e., for V between 0.001 and 0.1, the slip coefficient and number density are independent of V for a given l, while the drag coefficient is inversely proportional to V. We note that this range of V corresponds to plate velocities up to about 100 fps for gases at room temperature. It must be remembered, however, that the results are applicable to free molecule flow only, so that the effect of plate speed could be quite different at higher densities. Figure 2 shows the variation of the tangential momentum accommodation coefficient with l for $V \leq 0.1$. One interesting result is the disparity between the values of σ_s and σ_D. It is a common practice to determine the value of σ from a measured value of either C_s or C_D and then to use this value to calculate the other coefficient. The results of our analysis indicate that this procedure, which amounts to assuming that $\sigma_s = \sigma_D$, can lead to appreciable errors, especially if $L > d$.

Finally, the comparison between the calculated and experimental values of σ with the parameter l is physically reasonable for all cases investigated, although the calculated magnitudes of σ are generally lower than those found experimentally. Experimental values in excess of 0.9 have been found for a variety of surfaces,[1,2] although values as low as 0.6 have been reported.[3] By contrast, the calculated values of σ_D vary from 0.22 to 0.56 in the range $l = 0.8 - 1.2$ typical of most surfaces. This disparity is probably the result of several factors. First, there is the experimental difficulty, typified by the wide range of reported values for σ, of accurate control and determination of the state of the surface. Second, there is the theoretical idealization made here concerning the two-dimensional, single-crystal nature of the surface. The consequences of this assumption, unlike those of the immobility of the surface atoms, have not been discussed in detail in the literature. That the calculated accommodation coefficients are low relative to typical measured values suggests that the polycrystalline nature of real surfaces has an appreciable effect on tangential momentum transfer at gas-solid interfaces.

References

[1] Schaaf, S. A. and Chambré, P. L., "Flow of Rarefied Gases," *High Speed Aerodynamics and Jet Propulsion*, Vol. III, Princeton University Press, Princeton N. J., 1958, pp. 687–739.

[2] Hurlbut, F. C., "On the Molecular Interactions between Gases and Solids," HE-150-208, Nov. 1962, Institute for Engineering Research, Univ. of California, Berkeley, Calif.

[3] Hurlbut, F. C., "Influence of Pressure History on Momentum Transfer in Rarefied Gas Flows," *The Physics of Fluids*, Vol. 3, No. 4, July-Aug. 1960, pp. 541–544.

[4] Hurlbut, F. C., "Current Developments in the Study of Gas-Surface Interactions," *Rarefied Gas Dynamics, Fifth International Symposium*, Vol. 1, Academic Press, New York, 1967, pp. 1–34.

[5] Goodman, F. O., "Preliminary Results of a Three-Dimensional Hard-Spheres Theory of Scattering of Gas Atoms from a Solid Surface," *Rarefied Gas Dynamics, Fifth International Symposium*, Vol. 1, Academic Press, New York, 1967, pp. 35–48.

[6] McClure, J. D., "Atomic and Molecular Scattering from Solids: II. Comparison of Classical Scattering Models in Relation to Experiment," *Journal of Chemical Physics*, Vol. 51, No. 5, Sept. 1969, pp. 1687–1700.

[7] Yang, H. T. and Lees, L., "Rayleigh's Problem at Low Reynolds Number According to the Kinetic Theory of Gases," *Rarefied Gas Dynamics, First International Symposium*, Pergamon Press, London, 1958, pp. 201–238.

Relationship between Temperature and Velocity Profiles in a Turbulent Boundary Layer along a Supersonic Nozzle with Heat Transfer

L. H. Back* and R. F. Cuffel†
Jet Propulsion Laboratory, Pasadena, Calif.

Nomenclature

c_p = specific heat
c_f = friction coefficient, $(c_f)/(2) = (\tau)/(\rho_e u_e^2)$
H = enthalpy
M = Mach number
p = pressure
q = heat flux to wall
r = nozzle radius
r_c = throat radius of curvature
r_{th} = throat radius
St = Stanton number, $q/(H_{aw} - H_w)\rho_e u_e$
T = temperature
u = velocity parallel to wall

Received June 8, 1970. This work presents the results of one phase of research carried out in the Propulsion Research and Advanced Concepts Section of the Jet Propulsion Laboratory, California Institute of Technology, under Contract NAS7-100, sponsored by NASA.

* Member Technical Staff. Associate Fellow AIAA.
† Senior Engineer. Member AIAA.

u_τ = friction velocity, $[(\tau_w)/(\rho_w)]^{1/2}$
x = distance along wall
y^+ = dimensionless distance normal to wall, $(\rho_w u_\tau y)/(\mu_w)$
z = axial distance
α = thermal diffusivity
$\bar{\beta}$ = acceleration parameter
γ = specific heat ratio
ϵ_h = eddy diffusivity for heat transfer
ϵ_m = eddy diffusivity for momentum
θ = momentum thickness
μ = viscosity
ν = kinematic viscosity
ξ = coordinate along surface
ρ = density
τ = wall shear stress
Φ = energy thickness

Subscripts

aw = adiabatic wall condition
e = freestream condition
0 = reservoir condition
t = stagnation condition
w = wall condition

Introduction

IT has been realized for a long time that in either laminar or turbulent boundary layers in gas flows the Crocco relationship between total temperature and velocity profiles

$$(T_t - T_w)/(T_{te} - T_w) = u/u_e$$

does not apply in pressure gradient flows with heat transfer even if the wall is isothermal and the molecular or eddy diffusivities for momentum and heat transfer are equal or nearly equal. Instead, the relationship between the total temperature and velocity is generally expected to depend upon the degree of flow acceleration (or deceleration) and the amount of wall cooling (or heating), and may be influenced to some extent by the flow speed, i.e., compressibility effect when the molecular or eddy diffusivities are not the same.

In this Note the relationship between measured temperature and velocity profiles is presented for an accelerating, turbulent boundary-layer flow of air through a cooled, convergent divergent nozzle (Fig. 1). Boundary-layer measurements were made upstream, along the convergent section, and near the end of the divergent section where the flow is supersonic. These measurements span a relatively large flow speed range, the inlet and exit Mach numbers being 0.06 and 3.7, respectively. The operating conditions were such that the boundary layer remained essentially turbulent, i.e., laminarization did not occur in the accelerating flow.[1] The wall was cooled externally, the ratio of wall to stagnation temperature being 0.43–0.56.

The measurements are also related to current interest in the structure of very high speed turbulent boundary layers. For example, measurements are often made near the exit of supersonic nozzles with wall cooling (see the accumulation of available data shown in Ref. 2, Fig. 3 and other recent measurements Ref. 3–6). The present measurements provide information on the upstream history of the accelerating flow and on the relationship of upstream profiles to the profile near the nozzle exit.

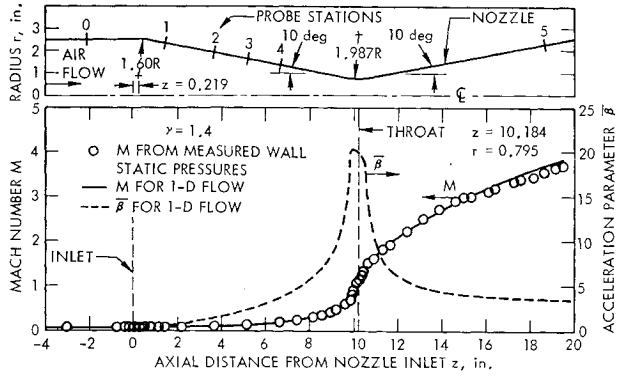

Fig. 1 Variation of Mach number and acceleration parameter $\bar{\beta}$ along a nozzle p_{t0} = 150 psia, T_{t0} = 1500°R.

PROBE POSITION	z in.	TEST	M_e	$\frac{d\left(\frac{\rho}{\rho_{t0}}\right)}{dx}$ in.$^{-1}$	$\frac{T_w}{T_{t0}}$	θ in.	$\frac{\rho_e u_e \theta}{\mu_e}$	$\frac{c_f}{2}$	$\frac{\phi}{\theta}$	$\frac{\phi}{\theta}$	St	$\frac{St}{c_f/2}$
0	-2.14	512	0.064	0	0.46	0.099	10,500	1.6 X 10^{-3}	0.117	1.18	1.86 X 10^{-3}	1.16
1	1.42	529	0.072	-0.0012	0.45	0.079	9,400	2.3 X 10^{-3}	0.109	1.39	1.76 X 10^{-3}	0.70
2	3.67	528	0.104	-0.0024	0.48	0.047	8,300	2.6 X 10^{-3}	0.100	2.13	1.84 X 10^{-3}	0.71
3	5.17	535	0.137	-0.0053	0.48	0.035	8,100	2.4 X 10^{-3}	0.095	2.73	1.78 X 10^{-3}	0.74
4	6.67	512	0.194	-0.014	0.50	0.030	9,600	2.3 X 10^{-3}	0.080	2.68	1.66 X 10^{-3}	0.76
5	18.65	554	3.57	-0.026	0.43	0.038	12,800	0.95 X 10^{-3}	0.108	2.83	0.63 X 10^{-3}	0.56

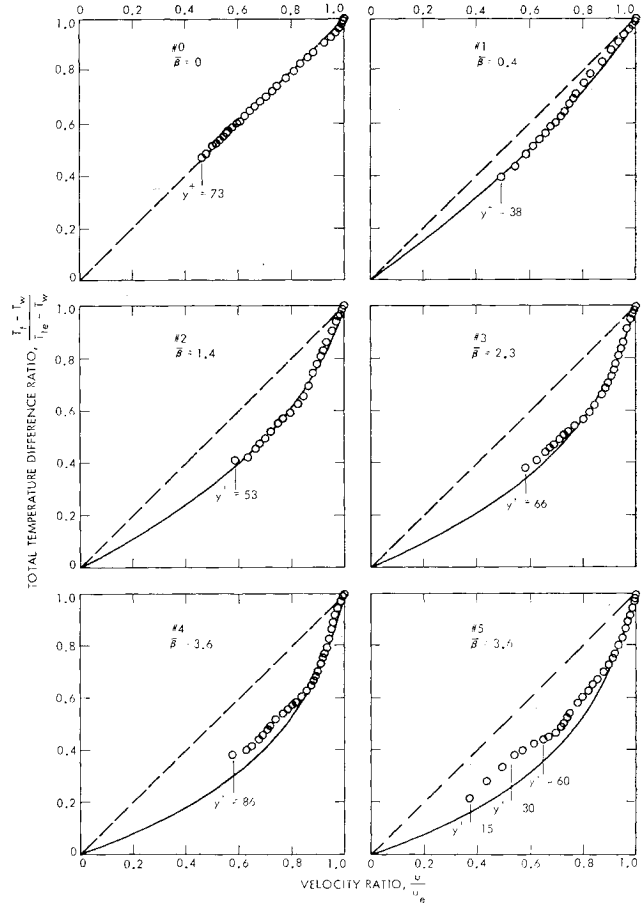

Fig. 2 Total temperature vs velocity profiles along the nozzle p_{t0} = 150 psia, T_{t0} = 1500°R: -- Crocco relation; — Laminar prediction Ref. 9; $\nu = \alpha$, $T_w/T_{t0} = 0.5$, $\mu\alpha T$, any flow speed.

Measurements

Boundary-layer surveys were made with a small flattened Pitot tube and with thermocouple probes. In the convergent section the thermocouple probe consisted of exposed bare wires; whereas a shielded aspirating thermocouple probe was used near the nozzle exit. Since the probes were in line axially, they were moved from one axial location to another from test to test. The Pitot tube was located 90° circumferentially from the temperature probe. Further description of the probes appears in Ref. 7. External measurements in-

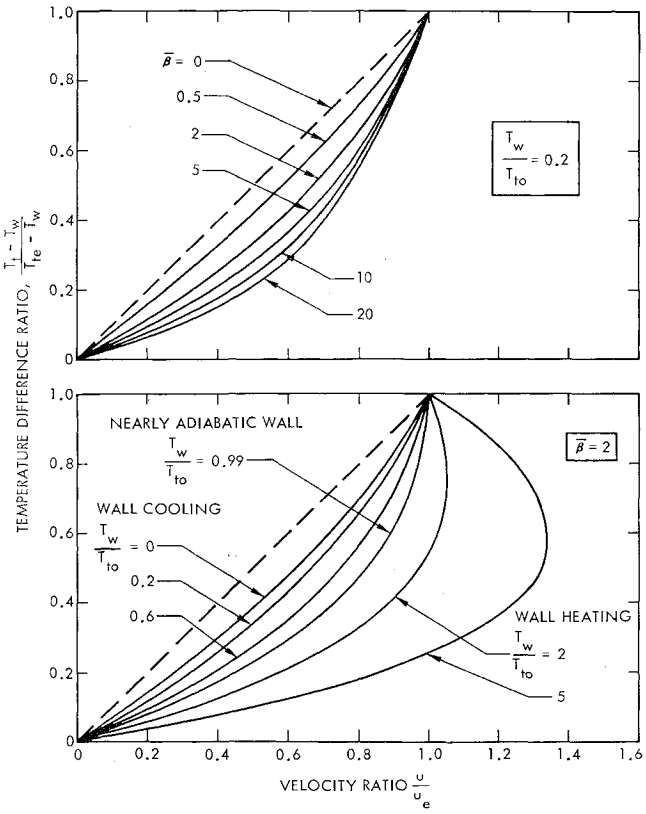

Fig. 3 Effect of acceleration and thermal boundary condition on total temperature-velocity relationship/Laminar prediction, $\nu = \alpha$, $\mu\alpha T$, any flow speed.

cluded wall static pressures and coolant-side wall temperatures. Semilocal values of wall heat fluxes were determined from calorimetric measurements. Confidence in the experimental temperature and velocity profiles was established by good agreement between the energy thicknesses computed from the profiles and those calculated by applying the energy integral relation along the nozzle by using the freestream flow variables determined from the pressure measurements, and the measured wall heat fluxes. The momentum integral relation was also found to check well along the convergent section where the boundary-layer measurements were close enough to be able to make a check, and the friction coefficient was estimated from the velocity profiles in the law of the wall region. Discussion of the individual velocity and temperature profiles and the other measurements including these checks is given in Ref. 7. The relationship between the temperature and the velocity profiles is discussed herein.

Results

Nondimensional total temperature vs velocity profiles are shown in Fig. 2. Upstream of the flow acceleration region (Station #0), the temperature-velocity relationship is essentially linear in the region where molecular transport is negligible. This correspondence implies that the eddy diffusivities for momentum and heat transfer are nearly equal, i.e., $\epsilon_m \cong \epsilon_h$ and for this situation the Crocco relation applies. The value of y^+ at the closest location to the wall is noted by the strike line. At locations within the viscous sublayer where molecular transport becomes important, the temperature profile would lie below the velocity profile because of the larger molecular diffusivity for heat than momentum transfer, i.e., $\alpha = (1/0.7)\nu$. This is not evident in Fig. 2 because of the height of the probes relative to the sublayer thickness, but is apparent at lower pressures where the measurements extend into the viscous sublayer.[8]

At subsequent stations in the acceleration region the temperature profiles lie below the velocity profiles at a given distance from the wall. In the representation of Fig. 2 the temperature-velocity relationship consequently bows progressively downward as one proceeds along the convergent section (stations 1, 2, 3, and 4). The departure of the measured total temperature and velocity profiles from the Crocco relation near the nozzle exit (station 5) where the Mach number is 3.6 is not much different than for the low speed profile in the convergent section (station 4) where the Mach number is 0.19.

The over-all behavior of the total temperature-velocity relationship beyond the viscous sublayer is very similar to that for a laminar boundary layer as indicated by the profiles shown in Fig. 2 by solid lines. These profiles were obtained from the locally similar solutions of Ref. 9 for a gas with equal molecular diffusivities for momentum and heat transfer, $\nu = \alpha$, i.e., Prandtl number of unity. The laminar profiles depend upon the acceleration parameter

$$\bar{\beta} = \frac{T_{t0}}{T_e}\frac{2\xi}{u_e}\frac{du_e}{d\xi} \quad \text{where} \quad \xi = \int_0^x \rho_e \mu_e u_e r^2 dx$$

and the amount of wall cooling T_w/T_{t0}, but not on flow speed since ν was taken equal to α. Thus the acceleration parameter $\bar{\beta}$, which varies along the nozzle as shown in Fig. 1, is a useful parameter that characterizes the relationship between temperature and velocity profiles in nozzle flow. It arises when either the laminar or turbulent boundary-layer equations are transformed by the Levy-Mangler transformation. Herein $\bar{\beta}$ was calculated for one-dimensional isentropic external flow[10]

$$\bar{\beta} = -\frac{(4/r)dr/dx}{(1 - M_e^2)}\bar{x}\left(\frac{T_{t0}}{T_e}\right) \quad \text{where} \quad \bar{x} = \left(\int_0^x \mu_e dx\right)\Big/\mu_e$$

The throat value is

$$\bar{\beta}_{th} = \frac{[2(\gamma + 1)]^{1/2}(\bar{x}_{th}/r_{th})}{(r_c/r_{th})^{1/2}}$$

Values of $\bar{\beta}$ at each of the probe locations are indicated in Fig. 2 and hence the influence of $\bar{\beta}$ on the shapes of the profiles is evident. Furthermore, at stations 4 and 5 values of $\bar{\beta}$ are the same even though the flow speeds are vastly different, and yet the profiles are nearly the same. This equivalence of profiles at the same value of $\bar{\beta}$ is evident for the turbulent boundary layer as shown by the data as it is for a laminar boundary layer as shown by the solid lines. Moreover, at each of the probe locations the eddy diffusivities ϵ_m and ϵ_h could not have been much different from one another in the turbulent boundary layer because of the general correspondence with the laminar profiles for which the molecular diffusivities are equal, i.e., $\nu = \alpha$. However, the laminar profiles are not expected to agree with the turbulent profiles in the viscous sublayer where molecular transport becomes important since there, $\nu \neq \alpha$. This is evident at station 5, where the boundary-layer measurements extend well into the viscous sublayer.

Heat-transfer results along with additional information related to the boundary layer appears in the table in Fig. 2. Values of the energy thickness are larger than the momentum thickness. Also in the acceleration region, the Stanton numbers St are smaller than the friction coefficients $c_f/2$, the ratio $St/(c_f/2)$ being about 0.7. These trends are consistent with predictions for laminar boundary layers, e.g., Ref. 9. However it is not correct to infer the important quantity $St/(c_f/2)$ from the laminar predictions, e.g., a value of 0.4 is predicted at $\bar{\beta} = 3$ whereas the experimental value of 0.7 for the turbulent boundary layer is considerably higher. This is because the temperature-velocity profile in the viscous sublayer of an accelerating turbulent boundary layer lies above that profile for laminar flow.

Because of the agreement between the laminar and measured turbulent boundary-layer profiles there is merit in indicating parametrically the effects of flow acceleration and thermal boundary condition on laminar boundary layers since the same trends may also be found in turbulent boundary layers in the region beyond the viscous sublayer. These predicted profiles are shown in Fig. 3. Even for a small value of $\bar{\beta}$ of 0.5, there is a noticeable difference from the Crocco relation. The profile at $\bar{\beta}$ of 20 would nearly correspond to the throat condition for the nozzle investigated (Fig. 1), but with a larger amount of wall cooling, i.e., $T_w/T_{t0} = 0.2$. With more wall cooling the profiles depart less from the Crocco relationship; the opposite is true for wall heating for which case the velocity profiles have overshoot, e.g., see Cohen and Reshotko.[11]

Summary and Conclusions

The measured relationship between the total temperature and velocity profiles in an accelerating turbulent boundary-layer flow through a nozzle was found to differ from the Crocco relation, with the amount of departure being dependent upon an acceleration parameter $\bar{\beta}$ which is related to nozzle shape. For accelerating flow the temperature-velocity relationship in the region beyond the viscous sublayer was similar to that for a laminar boundary layer and because of this correspondence, the eddy diffusivities for heat and momentum transfer ϵ_m and ϵ_h at each probe location are believed not to have differed much from each other. Based on the agreement between the laminar and measured turbulent boundary-layer profiles beyond the viscous sublayer, a rather large departure from the Crocco relation is expected because of flow acceleration and the thermal boundary condition, i.e., cooling or heating. From these observations it does appear that previous investigations of the structure of turbulent boundary layers made near the exit of nozzles could have been influenced to some extent by the pressure gradient that still existed at the location of interest and/or by the upstream history of the flow through the nozzle.

References

[1] Back, L. H., Cuffel, R. F., and Massier, P. F., "Laminarization of a Turbulent Boundary Layer in Nozzle Flow—Boundary Layer and Heat Transfer Measurements with Wall Cooling," *Transactions of the ASME: Journal of Heat Transfer*, to be published.

[2] Bushnell, D. M., et. al., "Comparison of Prediction Methods and Studies of Relaxation in Hypersonic Turbulent Nozzle-Wall Boundary Layers" *Symposium on Compressible Turbulent Boundary Layers*, SP-216, NASA, Dec. 1968, pp. 345–376.

[3] Kemp, J. H., Jr. and Sreekanth, A. K., "Preliminary Results from an Experimental Investigation of Nozzle Wall Boundary Layers at Mach Numbers Ranging from 27 to 47," AIAA Paper 69-686, San Francisco, Calif., 1969.

[4] Brott, D. L., et. al., "An Experimental Investigation of the Compressible Turbulent Boundary Layer with a Favorable Pressure Gradient," AIAA Paper 69-685, San Francisco, Calif., 1969.

[5] Bushnell, D. M. and Beckwith, I. E., "Calculation of Nonequilibrium Hypersonic Turbulent Boundary Layers and Comparisons with Experimental Data," AIAA Paper 69-684, San Francisco, Calif., 1969.

[6] Jones, R. A. and Feller, W. V., "Preliminary Surveys of the Wall Boundary Layer in a Mach 6 Axisymmetric Tunnel," TN D-5620, Feb. 1970, NASA.

[7] Back, L. H. and Cuffel, R. F., "Turbulent Boundary Layer and Heat Transfer Measurements Along a Convergent-Divergent Nozzle," to be published.

[8] Back, L. H., Cuffel, R. F., and Massier, P. F., "Effect of Wall Cooling on the Mean Structure of a Turbulent Boundary in Low-Speed Gas Flow," *International Journal of Heat and Mass Transfer*, Vol. 13, No.6, June 1970, pp. 1029–1047.

[9] Back, L. H., "Acceleration and Cooling Effects in Laminar Boundary Layers—Subsonic, Transonic, and Supersonic Speeds," *AIAA Journal*, Vol. 8, No. 4, April 1970, pp. 794–802.

[10] Back, L. H. and Witte, A. B., "Prediction of Heat Transfer from Laminar Boundary Layers, with Emphasis on Large Free-Stream Velocity Gradients and Highly Cooled Walls," TR 32-728, June 1965, Jet Propulsion Lab., Calif.

[11] Cohen, C. B. and Reshotko, E., "Similar Solutions for the Compressible Laminar Boundary Layer with Heat Transfer and Pressure Gradient," R-1293, 1956, NACA.

Parametric Differentiation Method to Structural Optimization Problems

A. V. Setlur* and M. P. Kapoor*
Indian Institute of Technology, Kanpur, India

A STRUCTURAL optimization problem can be cast as a mathematical programing problem in the form,

$$\min f(\mathbf{X}) \tag{1}$$

subject to

$$g_j(\mathbf{X}) \leq 0 \quad j = 1, \ldots, m$$

where $\mathbf{X}$ is a n-dimensional vector of design variables x_i, $i = 1, 2, \ldots, n$ and $g_j(\mathbf{X})$ are the given constraints on the design. The function $f(\mathbf{X})$ is called the objective function and its choice is governed by the nature of the problem. One of the methods to obtain the solution of the constrained minimization problem Eq. (1) is to solve a sequence of unconstrained minimization problems of the form,

$$\Phi(\mathbf{X},r) = f(\mathbf{X}) - r \sum_{j=1}^{m} \frac{1}{g_j(\mathbf{X})} \tag{2}$$

where Φ is the penalty function and r is an *arbitrary* penalty parameter which in the limit goes to zero. Solution to several structural optimization problems[1,2] has been successfully obtained by the sequential minimization of the penalty function Φ. However, the discrete numerical values chosen for the penalty parameter r influences the rate of convergence of this method.[3,4]

This Note presents a parametric differentiation approach to obtain the solution of Eq. (1). This is achieved through the minimization of the function $\Phi(\mathbf{X},r)$ where $\mathbf{X}$ is now treated to be a function of the continuous parameter r. The unconstrained minimization problem is transformed by the classical calculus approach to a set of simultaneous nonlinear algebraic equations. The latter, in turn is transformed to a set of simultaneous linear differential equations with variable coefficients. The resulting initial value problem in ordinary differential equations can be solved numerically to find $\mathbf{X}(r)$ for $r = 0$ in order to give the solution of Eq. 1. The convergence to the solution is geared to the uniqueness of the associated first order initial value problem and thus is guaranteed. This method ensures that the solution so obtained is only a stationary point. In order to satisfy that the solution is a minimum of Eq. (2), the matrix of second partials of Φ function at the solution should be positive definite. No additional efforts are required to formulate the matrix of the second partials of Φ. This is obtained from a part of the algorithm proposed here. A method is indicated to test the positive definiteness of this matrix which ensures the solution to Eq. (1).

The numerical experimentation on the proposed method for structural optimization problems is in progress.

Received April 2, 1970; revision received July 28, 1970.

* Assistant Professor, Department of Civil Engineering.